

Evaluation of Ride-Sourcing Search Frictions and Driver Productivity: A Spatial Denoising Approach

Natalia Zuniga-Garcia^{a,b}, Mauricio Tec^b, James G. Scott^{b,c}, Natalia Ruiz-Juri^d, Randy B. Machemehl^a

^a*The University of Texas at Austin, Department of Civil, Architectural and Environmental Engineering, 301 E. Dean Keeton St. Stop C1761, Austin, TX 78712, United States*

^b*The University of Texas at Austin, Department of Statistics and Data Sciences, 2317 Speedway Stop D9800, Austin, TX 78712, United States*

^c*The University of Texas at Austin, Department of Information, Risk, and Operations Management, 2110 Speedway Stop B6000, Austin, TX 78705, United States*

^d*The University of Texas at Austin, Network Modeling Center, Center for Transportation Research, 3925 West Braker Lane Austin, TX 78759, United States*

Abstract

This paper considers the problem of spatial and temporal mispricing of ride-sourcing trips from a driver perspective. Using empirical data from more than 1.1 million rides in Austin, Texas, we explore the spatial structure of ride-sourcing search frictions and driver performance variables as a function of the trip destination. The spatial information is subject to noise and sparsity, and researchers tend to aggregate the data in large areas, which results in the loss of high-resolution insights. We implemented the graph-fused lasso (GFL), a spatial smoothing or denoising methodology that allows for high-definition spatial evaluation. GFL removes noise in discrete areas by emphasizing edges, which is practical for evaluating zones with heterogeneous types of trips, such as airports, without blurring the information to surrounding areas. Principal findings suggest that there are differences in driver productivity depending on trip type and pickup and drop-off location. Therefore, providing spatio-temporal pricing strategies could be one way to balance driver equity across the network.

Keywords: ride-sourcing, emerging mobility, search frictions, spatial pricing, data analysis, spatial smoothing

1. Introduction

Ride-sourcing companies, also known as transportation network companies (TNCs), provide pre-arranged or on-demand transportation service for compensation [1]. They operate as a two-sided market that connects drivers of personal vehicles with passengers. TNCs have been controversial in different cities around the world due to multiple factors, such as the perception that they are unfair competition to taxi services, and lack of regulation of their

Email addresses: nzuniga@utexas.edu (Natalia Zuniga-Garcia), mauriciogtec@utexas.edu (Mauricio Tec), james.scott@mcombs.utexas.edu (James G. Scott), nruizjuri@mail.utexas.edu (Natalia Ruiz-Juri), rbm@mail.utexas.edu (Randy B. Machemehl)

pricing system, and driver selection. Pricing strategies for TNCs has been criticized due to concerns for the welfare of providers and consumers [2]. A desirable characteristic of a ride-sourcing platform is that two drivers in the same location at the same time do not envy each other’s future income [3]. However, trips may be mispriced relative to other trip opportunities, leading to inefficiencies on a network level. First, incorrect pricing results in loss of service reliability because drivers may select a specific kind of trip or decline to to accept trips from particular locations, destinations, or time frames. Second, arbitrary driver earnings can limit long-term driver participation, reducing the service supply through limited driver availability.

Recent research efforts have addressed ride-sourcing’s spatial mispricing problem by proposing different pricing strategies and driver-passenger matching functions. The primary goal is to reduce search frictions, the imbalance between driver supply and passenger demand across geographic areas that causes the presence of high matching and reaching times¹. Some examples include incorporating spatial surge pricing models [4, 5], spatio-temporal pricing mechanisms [3], search and matching models [6, 7, 8, 9], and non-linear pricing models [10]. However, the majority of the methods focused on the optimization of the platform revenue and do not evaluate the driver perspective. There is also limited evidence on the driver opportunity cost of the trip destination. Research on spatial pricing suggests that accounting for prices based on both origin and destination does not provide a substantial gain when optimizing for platform revenue [5]. But, other authors have demonstrated with simulation how a spatio-temporal pricing mechanism can result in higher social (consumer and provider) welfare when using a model based on origin and destination prices that preserves driver equity [3].

Furthermore, there is a lack of understanding of the spatial structure of driver productivity² and limited empirical evaluations. In this research, we study the spatial variation of driver productivity and search frictions using empirical data from a ride-sourcing company. Analyzing operational and performance variables at a high-definition spatial level requires additional data analytics methods. If sub-areas contain few data points or no data at all, it is unwise to rely on separate analyses conducted at each location. The lack of sufficient data in some sub-areas could mean that those independent estimates are subject to extreme noise or may be impossible to obtain. The problem of noisy estimates grows as space is discretized more finely since the availability of data at each sub-area will decrease further. In the literature related to the pricing issue, some studies do not account for the spatial heterogeneity of the variables [11, 12, 2], while others incorporate it in a highly aggregate manner [4, 7, 6]. We propose the use of a spatial smoothing or denoising technique that allows a fine-resolution analysis, compensates for inherent sampling noise, and enhances interpretability. With spatial smoothing, very fine discretization of space can be used. The proposed method uses spatial aggregation at the traffic analysis zone (TAZ)³ level and smooths the value of all TAZs jointly

¹Market frictions are those factors that prevent the market clearing, leaving some buyers and sellers unable to immediate trade as both may need to invest in a costly search process to locate matching partners. Search frictions are present in ride-sourcing markets as a consequence of the spatial mis-allocation of drivers and passengers; often drivers are in one place and passengers in another

²We define the driver productivity in terms of profit per unit time.

³The TAZs are the unit of geography most commonly used in conventional transportation planning models.

via a convex optimization routine.

Spatial smoothing is useful when multiple samples of varying sizes are taken from spatially connected locations, and the parameters of interest are correlated spatially. The term “smoothing,” although widely used, is a misnomer; not all types of smoothing seek the same purpose. Some applications, like Gaussian smoothing, average a point over its neighboring values using a set of distance-depending weights, or kernels, thus removing noise by blurring. When there are natural drastic changes between sub-areas or “edges,” the magnitude of the change will be dissipated to the nearby sub-areas. The smoothing technique we use in this research, known as total variation denoising or fused lasso, has the opposite goal: to remove noise by emphasizing edges. This type of smoothing has been used successfully for signal detection and edge-preserving image denoising [13, 14]. This approach is more appropriate to transportation studies where there are areas with high densities of heterogeneous trips, such as an airport area, and researchers would like to emphasize the boundaries instead of blurring the information to surrounding areas.

The principal objective of this research is to analyze the spatial structure of ride-sourcing operational and driver performance variables to support the need for new pricing strategies. We identify different productivity metrics and aggregate the variables in space and time to evaluate spatio-temporal changes. Further, we focus on driver productivity as a function of the opportunity cost of trip destination. We make use of the graph-fused lasso (GFL) spatial smoothing technique and provide an empirical analysis of ride-sourcing markets using data made available by an Austin-based TNC company, including trips during the period that Uber and Lyft, the principal TNC companies, were temporarily out of the city⁴.

The main contributions of this study include: (i) empirical evidence of spatial and temporal variation of driver productivity variables as a function of trip destination; (ii) a temporal and spatial evaluation of different ride-sourcing operational measures and search frictions in Austin; (iii) implementation of a spatial denoising methodology to analyze high-definition spatial variables; and (iv) verification of the usefulness of recent developments in big data analytics to solve transportation problems.

Subsequent sections of the paper are organized as follows: Section 2 provides a literature review of the principal aspects of pricing strategies in ride-sourcing markets; Section 3 provides a description of the dataset and implemented metrics; Section 4 presents the selected smoothing method; Section 5 includes the empirical analysis and provides results and discussion; and finally, Section 6 contains conclusions and final remarks.

2. Literature Review

This section summarizes prior related research on pricing strategies, spatial pricing, and spatial aggregation in ride-sourcing systems.

The popularity of ride-sourcing platforms relies not only on the advanced technology of connecting users and providers through cell phone applications but also on the pricing strategies. An essential tool used by TNCs is dynamic (or surge) pricing that helps in

⁴Uber and Lyft left the city from May 2016 to May 2017 after the Austin City Council passed an ordinance requiring ride-hailing companies to perform fingerprint background checks on drivers, a stipulation that already applies to Austin taxi companies [15].

managing both supply and demand. Surge pricing consists of raising the cost of a trip when demand outstrips supply within a fixed geographic area. The existing literature on pricing mainly addresses the problem of dealing with temporal demand fluctuations at a given location. Recent research in price strategies has been focused on comparing the impact of static versus dynamic prices and analyzing benefits, as in Castillo et al. [16], Zha et al. [11], Banerjee et al. [12], Cachon et al. [2]. Authors agree on the benefits of dynamic pricing to both users and providers [16, 2] and the need for regulation [17, 11]. Additional research has been dedicated to studying pricing policies and effects on the labor supply (or drivers’ choice of hours), such as by Zha et al. [17], Sheldon [18], Chen and Sheldon [19]. In the context of ride-sourcing trips, labor supply elasticities have substantial implications on the effectiveness of surge pricing because the temporary increase in wages can have an immediate effect on whether or not drivers continue to work.

Research that incorporates the spatial distribution of demand and supply in ride-sourcing system pricing schemes is recent. Authors have attempted to balance spatial supply-demand using different mechanisms. For example, He et al. [4] studied pricing and penalty strategies for platform revenue maximization and social welfare optimization in a hybrid (street-hailed taxi and ride-sourcing) market with variable demand across space. Bian [6] and Buchholz [7] modeled the passenger search and driver matching process using a hybrid market [6] and only taxis [7], and evaluated their models using empirical information. Zha et al. [8] proposed a geometric matching method for ride-sourcing systems based on market equilibrium and assuming a revenue maximization platform. They suggest the use of a rate cap regulation to avoid excessively high pricing and provide an empirical study using data from a Chinese TNC. Also assuming platform revenue maximization, Castro et al. [9], Afèche et al. [20], Bimpikis et al. [5] considered the problem of matching ride-sourcing costumers to “strategic” drivers in a geometric area by examining how the platform should respond to a short-term [9] and long-term [20, 5] supply-demand imbalance. Drivers are considered strategic because they move in equilibrium in a simultaneous move game, choosing where to reposition based on prices, supply levels, and driving costs.

For this study, the work by Ma et al. [3] is relevant. They addressed spatial and temporal variations using origin-destination prices that warranty driver equity. The authors proposed a spatio-temporal pricing (STP) mechanism that considers multiple locations and time periods along with rider demand, willingness to pay, and driver supply varying over space and time. They show with simulation that this mechanism provides higher social welfare than the static origin-based pricing scheme. Bimpikis et al. [5] also analyze pricing models using origin-destination prices. The authors found that if the demand pattern is not balanced, the platform can benefit substantially from pricing rides differently depending on the origin location. They discovered that the benefit of origin-destination pricing is not as significant as origin-based pricing regarding the maximization of platform revenue.

Incorporating spatial information is a complex challenge. First, the availability of empirical ride-sourcing data is limited. Thus, some authors relied on simulations [3, 5] or limit their research to taxi-only data [4, 7]. Second, when available, spatial information is subject to noise and high sparsity, so researchers tend to aggregate the data in large areas losing valuable high-resolution insights. Further, data processing does not include spatial denoising steps. Examples include He et al. [4] who summarized the demand pattern of a taxi network in Beijing using eighty-one squared-area zones of 5.4 km^2 to model pricing and penalty

strategies. With the objective of modeling the search and matching process, Buchholz [7] aggregated NYC taxi data in thirty-nine zones conformed by uniting census tracks, and Bian [6] summarized Uber and taxi information in NYC using forty geographic locations. In our work, we summarized ride-sourcing information in a total of 1,305 traffic analysis zones (TAZs) in Austin, Texas. TAZ areas vary from 0.01 km^2 in the Central Business District (CBD) to 30 km^2 in the rural area, with an average of 2 km^2 .

This paper’s primary contribution to current literature encompasses the use of spatial smoothing techniques to evaluate high-definition denoised spatial information. Our work is focused on providing empirical proof of space and time heterogeneity of driver performance and other ride-sourcing operational variables. To date, pricing mechanisms are mainly focused on maximizing platform revenue, minimizing the evaluation of driver productivity. But drivers are an essential part of the success of ride-sourcing systems, and the provision of fair working conditions can result in more reliable services.

3. Methodology

This section provides a description of the dataset and the principal variables and metrics used in the analysis.

3.1. Ride-Sourcing Data

We used a dataset that an Austin-based TNC (Ride Austin) made available in early 2017 [21]. It consisted of 1,494,125 rides between June 2, 2016, and April 13, 2017. Each trip corresponds to a row in the database. The dataset provides a description of the trip, rider, and driver (anonymized), payment, cost, among other trip information. Because demand during the first few months was limited, we focused our analysis on data from September 1, 2016, to April 13, 2017. We selected rides with origin and destination coordinates within the Austin TAZs. Our analysis includes only regular car category trips; we omitted trips by sport-utility vehicles (SUVs), premium, and luxury vehicle categories because the fare rate is different in each case. Similarly, we analyzed only flat-rate trips, i.e. trips that do not include any surge price. The total number of rides examined after the restrictions was 1,117,943 rides, with approximately 5,000 average daily trips.

3.1.1. Space Discretization

Space discretization consists of summarizing the trip variables within the origin or destination TAZ using the average value. We matched the trip pick-up (origin) and drop-off (destination) longitude and latitude coordinates with corresponding TAZ location. The mean count of trips per TAZ was 1,000. The Austin-Bergstrom International Airport (ABIA) TAZs presented the highest demand with 58,803 origin trips and 75,941 destination trips. Figure 1 (a) illustrates TAZs in the Austin area and provides the location of the TAZs corresponding to the ABIA area. For a specific case study, we selected trips with origins inside the Austin downtown CBD, using the area type TAZ classification. CBD trips correspond to a total of 176,219 origin trips, approximately 16 percent of the total evaluated rides. Figure 1 (b) provides a spatial description of Austin area types, and 1 (c) presents a detailed view of the downtown area.

3.1.2. Time Discretization

Time discretization is based on system peak hours because these correspond to higher travel time and delays. We used four different time classifications. First, we divided the trips into weekdays and weekend trips. Then, the weekday trips were split into AM-peak (from 6 to 9 AM), PM-peak (from 4 to 7 PM), and off-peak hours.

3.2. Description of Variables

We selected different measures as indicators of driver performance. Specifically, we focused on operational variables such as trip fare, trip distance, and search frictions (waiting or idle time and reaching time). Additionally, we estimated three different productivity variables based on trip fare and driver time.

3.2.1. Operational Variables

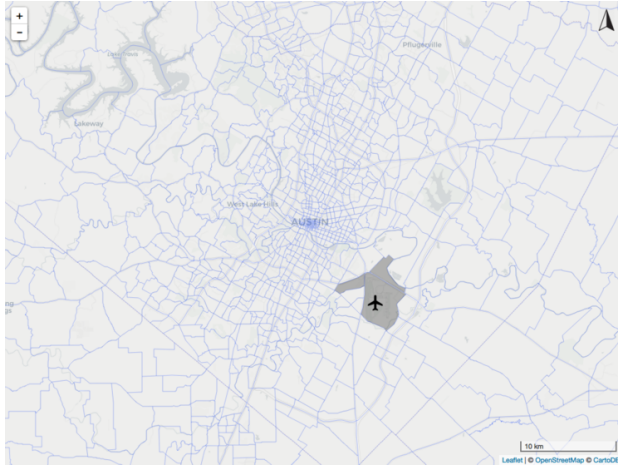
Among operational variables, we selected trip fare, which corresponds to the total passenger cost excluding tip, roundup amount⁵, and other operational fees like booking and airport fees. Trip fare consists of the sum of base fare, time rate, and distance rate; and the minimum fare is \$4 (see Equation 1) in the regular car category.

$$fare_{trip} = \max(base\ fare + distance\ rate + time\ rate, 4) \quad (1)$$

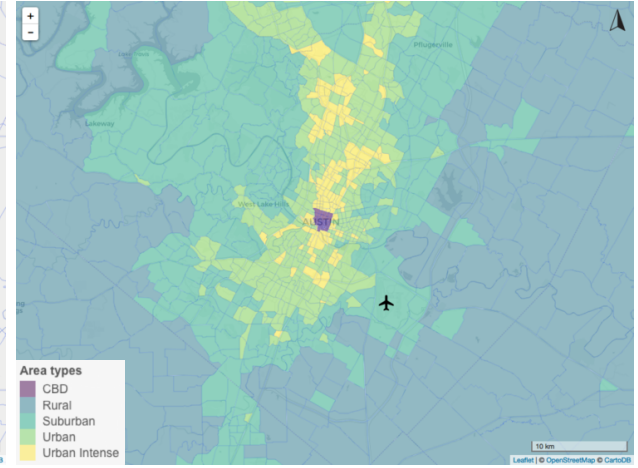
The trip distance used represents the distance in kilometers from the pick-up to the drop-off location provided in the database. Reach time, which was also provided in the database, corresponds to the time it took the driver to reach the rider after the trip was assigned to him. The idle time was estimated based on the driver's unique identification information and corresponds to the time between the previous trip drop-off time and the next trip pick-up time. We only considered idle times lower than sixty minutes in the analysis to avoid including other driver activities. The mean idle time was eighteen minutes, with a standard deviation of 13.7 minutes. Figure 2 provides a driver time diagram with a graphical representation of the variables. We can describe the driver time values as follows:

- t_0 : time $trip_1$ started at the pick-up location
- t_1 : time $trip_1$ finished at the drop-off location
- t_2 : time $trip_2$ is assigned to the driver
- t_3 : time $trip_2$ started at the pick-up location
- t_4 : time $trip_2$ finished at the drop-off location

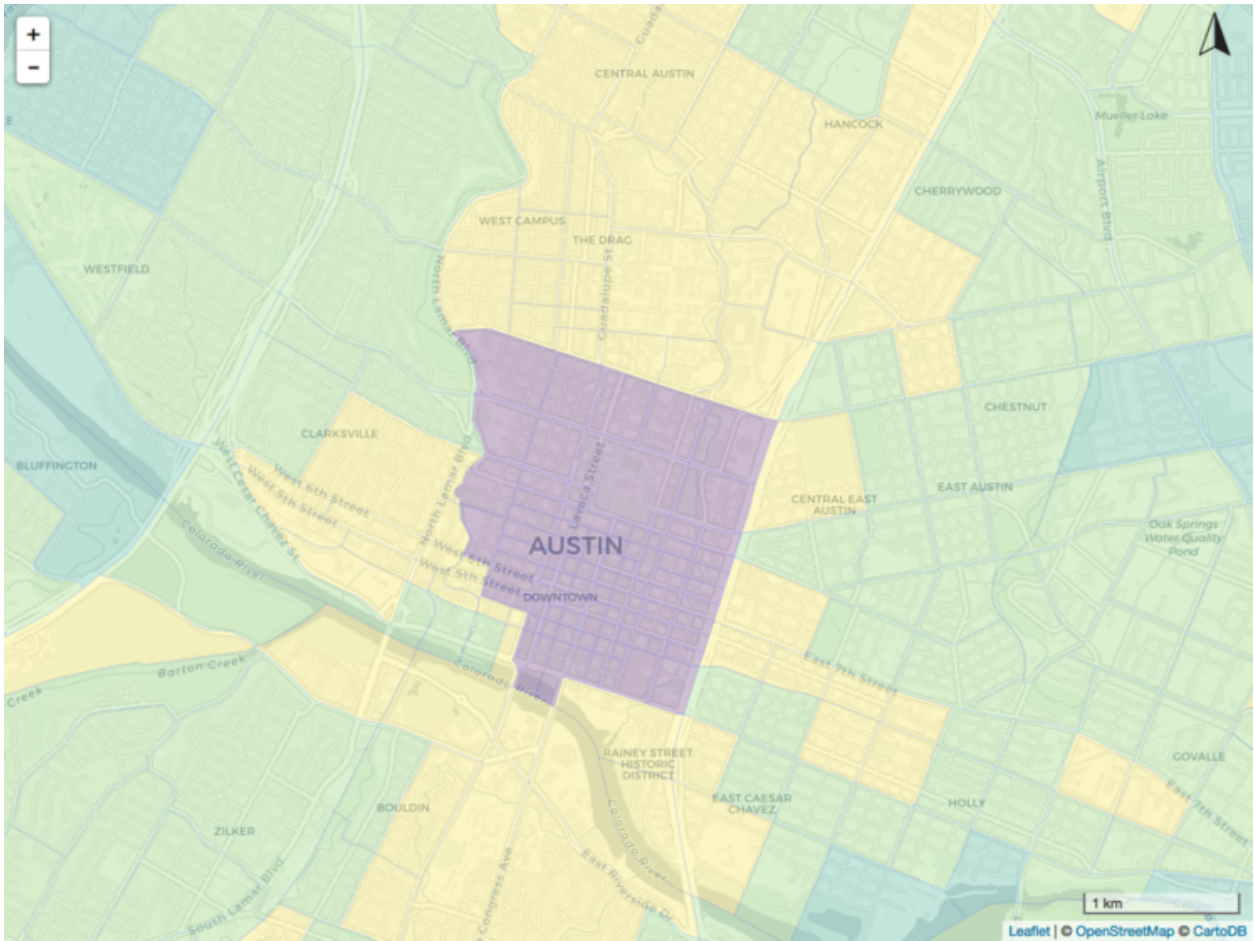
⁵Ride Austin allows riders to round up the total fare to the nearest dollar and designate it to a local charity.



(a) TAZs in Austin (airport TAZs shaded)



(b) TAZ area types



(c) TAZ area types (downtown)

Figure 1: Description of TAZs

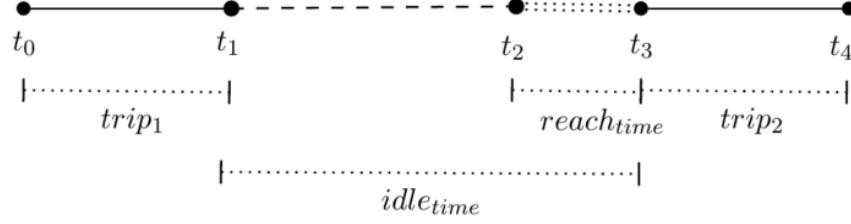


Figure 2: Driver time diagram

Using the driver time description, we estimated the idle time and the reach time using Equations 2 and 3, respectively.

$$reach_{time} = t_3 - t_2 \quad (2)$$

$$idle_{time} = t_3 - t_1 \quad (3)$$

3.2.2. Productivity Variables

We estimated three different productivity variables based on the driver time diagram. Productivity A corresponds to the throughput of the $trip_1$ in dollars per hour, estimated using Equation 4. Productivity B refers to the productivity of the $trip_1$ including the idle time after finishing that trip, estimated using Equation 5. Finally, Productivity C corresponds to the productivity of two consecutive trips including the idle time between them. This metric is an indirect measure of the continuation payoff intended to capture the opportunity cost of the destination location, estimated using Equation 6. The primary objective of evaluating these variables is to analyze the impact of trip destination on driver productivity; thus we only considered two consecutive trips.

Productivity A captures only the revenue of a trip divided by its duration, so it is not expected to obtain the effect that ending a trip in a region of low density may have. Productivity B adds idle time after the end trip to the formula; in this way, it penalizes drivers for traveling to low-demand zones. Productivity C also includes the revenue and duration of the following trip, seeking to capture further spatial dynamics for ending in a specific region.

$$Productivity \text{ A} = \frac{fare_{trip_1}}{t_1} \quad (4)$$

$$Productivity \text{ B} = \frac{fare_{trip_1}}{t_3} \quad (5)$$

$$Productivity \text{ C} = \frac{fare_{trip_1} + fare_{trip_2}}{t_4} \quad (6)$$

4. Spatial Smoothing Approach

Spatial smoothing techniques are typically used for a wide range of applications. For example, in the image processing field smoothing approaches are used for image denoising [22]; in computational geometry and object modeling, to reconstruct surfaces [23, 24]; and, in machine learning, to impute missing values [25]. Other applications include spatial statistical analysis. For instance, predicting crime hotspots by smoothing incident report locations [26], detecting crash hotspots using historical crash data [27], or event detection using taxi trips [28].

4.1. Background

Space can be modeled as continuous or discrete. Smoothing techniques for the continuous case include Gaussian processes, Gaussian kernel smoothing, and continuous random fields, while for the discrete case some methods include Graph kernel smoothing and Graph Laplacian smoothing. Spatial-smoothing techniques can be classified into local and global approaches [29], where local approaches smooth only a local window around each point, such as neighboring pixels in an image, while global methods typically define an objective function over the entire graph and simultaneously optimize the whole set of points. The most simplistic local approaches simply replace each point with the average or median of the points in its window [29].

An important aspect of using spatial data is specification of the spatial covariance function. Data can be isotropic, meaning that the spatial dependence does not depend on the direction of the spatial separation between sampling locations, only on the distance [30]. Methods such as the Gaussian kernel assume isotropy. However, this assumption is often violated by real-world data, where arbitrary discontinuities may be present. In some cases, it is more appropriate to rely on anisotropic smoothing techniques, which can smooth differently in distinct directions and locations. Anisotropic local methods for images include bilateral filter and guided filter used to preserve edges. Global techniques for anisotropy include discrete Markov random fields (MRFs). This method defines a joint distribution over a graph via a product of exponentiated potential functions over cliques, or as a conditional autoregressive (CAR) model where each node’s unnormalized likelihood is written conditioned on all other nodes in the graph [29].

An alternative to MRFs for global smoothing is the graph-based trend filtering (GTF) [28], which is a special use of the generalized lasso [31] that applies an ℓ_1 penalty⁶ to the vector of $(k + 1)^{st}$ -order differences, where the integer $k \geq 0$ is a hyperparameter. While global approaches like MRFs and GTF typically yield better results, they often fail to scale to large graphs because every node being dependent on the rest of the graph [29]. One exception is a particular case of the GTF with $k = 0$, known as graph-based total variation denoising, also called graph-fused lasso (GFL).

4.2. Graph-Fused Lasso

In spatial smoothing, the underlying statistical model can be represented as shown in Equation 7. Assume that we have observations y_i , each associated with a vertex $s_i \in \mathcal{V}$ in an undirected graph $\mathcal{G} = (\mathcal{V}, \mathcal{E})$ with node set \mathcal{V} and edge set \mathcal{E} . The edge set determines which sites are

⁶Formally, the ℓ_p -norm of x is defined as: $\|x\|_p = \sqrt[p]{\sum_i |x_i|^p}$, where $p \in \mathbb{R}$.

neighbors on the graph. The goal of the smoothing techniques is to estimate x_i in a way that leverages the assumption of spatial smoothness over the underlying graph. One way to estimate x is by using the GFL, defined by a convex optimization problem that penalizes the first differences of the signal across edges.

$$y_i = x_i + \epsilon_i, \quad i = 1, \dots, n, \quad (7)$$

where, x_i is the “true” denoised signal and ϵ_i is mean-zero error.

The GFL smoothing problem can be represented using Equation 8. The first term corresponds to a smooth convex loss function and the second term is the ℓ_1 penalty that rewards the solution for having small, absolute first differences across edges in the graph. Equation 8 does not have a closed-form solution. Therefore, convex optimization approaches such as the alternating direction method of multipliers (ADMM)⁷ [32] are required. Many efficient, specialized procedures using ADMM have been developed, as by Wahlberg et al. [33], Barbero and Sra [34], and Tansey and Scott [35]. We implemented the method developed by Tansey and Scott [35], which leads to an efficient approach that presents a fast solution and is also scalable. [Appendix A](#) provides more details of the method.

$$\underset{\mathbf{x} \in \mathbb{R}^n}{\text{minimize}} \quad \ell(\mathbf{y}, \mathbf{x}) + \lambda \sum_{(r,s) \in \mathcal{E}} |x_r - x_s|, \quad (8)$$

where, ℓ is the loss function, r is the start node and s the end node, $n = |\mathcal{V}|$, and $\lambda > 0$ is the regularization parameter.

4.2.1. Loss Function

In this study, we selected a penalized weighted least squared-error loss function to take into account the differences in the number of observations within each zone. Let us denote by η_i the count of trips observed within the i -th TAZ, then the objective function takes the form:

$$\underset{\mathbf{x} \in \mathbb{R}^n}{\text{minimize}} \quad \sum_{i=1}^n \frac{\eta_i}{2} (y_i - x_i)^2 + \lambda \sum_{(r,s) \in \mathcal{E}} |x_r - x_s| \quad (9)$$

The justification for this set of weights is the following. If $(y_{i,1}, \dots, y_{i,\eta_i})$ are the observations in the i -th TAZ, $(x_{i,1}, \dots, x_{i,\eta_i})$ the predicted values, then the squared error of the full model would be:

$$\frac{1}{2} \sum_{i=1}^n \sum_{j=1}^{\eta_i} (y_{ij} - x_{ij})^2 \quad (10)$$

And if in the above formula we replace all the y_{ij} and x_{ij} with their means y_i and x_i , then we recover the squared-error term of (9).

4.2.2. Choosing the Regularization Parameter

The regularization parameter λ controls the amount of smoothing. With $\lambda = 0$, no smoothing is done, and as $\lambda \rightarrow \infty$, the estimated values become the same in every location. To select

⁷The ADMM is an algorithm that solves convex optimization problems by breaking them into smaller pieces, each of which is then easier to handle.

the optimal λ for each variable, we first randomly split the data into a training and a test set of respective sizes 90 percent and 10 percent. Then, we used the training set to estimate the smoothed value of each region using different values of λ ranging from 0.001 to 100. For a new data point outside the training set, the prediction would be the smoothed value of the region where it was observed. The predictions of the test data are used to estimate the out-of-sample prediction error using the root mean square error (RMSE) criterion, described by Equation 11. The optimal λ corresponds to the minimum RMSE from the possible λ values tested and it is the amount of smoothing that best filters the noise and represents what we would expect from a newly observed point. After selecting the best λ , we obtained the final estimates rerunning the model with the optimal λ using both the training and test data.

$$\widehat{RMSE} = \left(\frac{1}{\sum_{i=1}^n \eta_i} \sum_{i=1}^n \sum_{j=1}^{\eta_i} (y_{ij} - \hat{x}_i)^2 \right)^{1/2}, \quad (11)$$

where n and η_i are the number of TAZ regions and counts for the i -th TAZ from the test set, and \hat{x}_i is the prediction for the i -th TAZ obtained from the training data.

4.2.3. Graph Definition

The edges for joining the TAZ nodes were chosen according to a k -nearest neighbors principle. The location of a TAZ was computed as the mean longitude and latitude of all the points observed in that region. Once the node locations were calculated, an edge (r, s) was added for all s within the k -nearest neighbors of each node r . We used $k = 4$ so that the graph represented spatial adjacency. We remark that there was little variation in the final results for other close values of k .

4.2.4. GFL Denoising Example

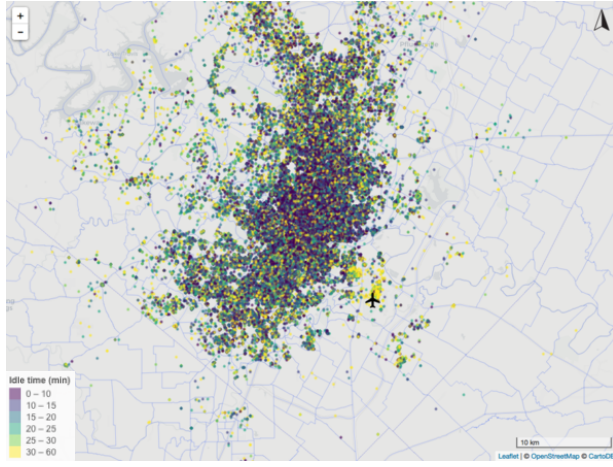
Figure 3 shows examples of the application of the GFL smoothing to the variables of interest. The first image presents the raw data points, where each dot in the map represents the origin of a trip. The next image provides the information summarized per TAZ. Finally, the third image presents the denoised graph. The denoised image allows a better interpretation of the spatial distribution of the variables. Also, we can observe a clear example of the ℓ_1 penalty benefits in the airport area of Figure 3 (e), corresponding to the idle time variable. The GFL preserves the high contrast of values in this area and keeps it independent of the surrounding area values.

5. Results and Discussion

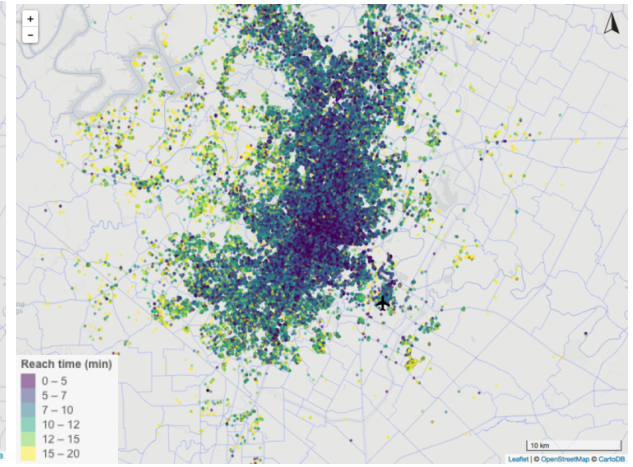
This section presents the principal results and discussion of the main findings.

5.1. Operational Variables

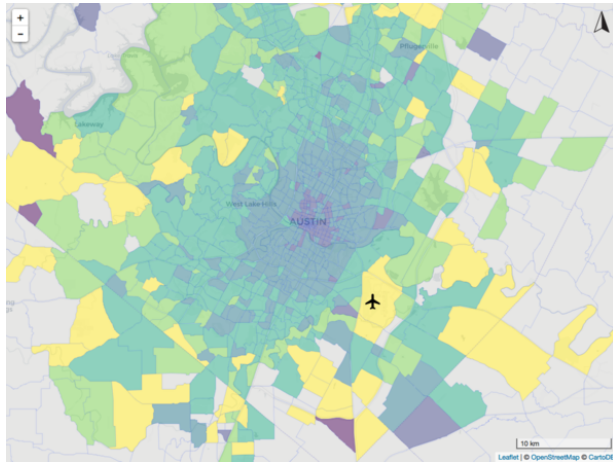
Operational variables, including trip distance and search frictions, are analyzed based on the origin (pick up) TAZ of the trips. Results are shown in Figure 4. The resulting maps of trip distance spatial distribution indicate that the majority of short trips are concentrated in the central area, while longer trips originate from the urban sectors. Additionally, trip distances do not show significant changes across the analyzed time frames. The main difference is



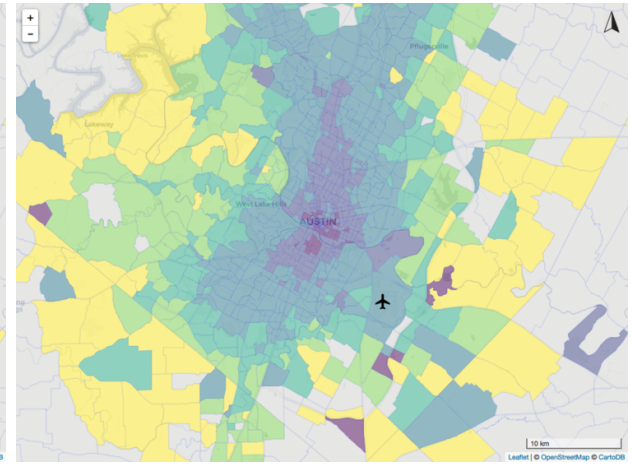
(a) Idle time data points



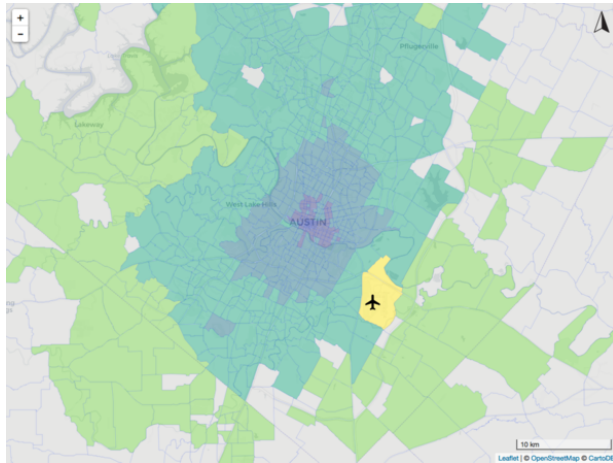
(b) Reach time data points



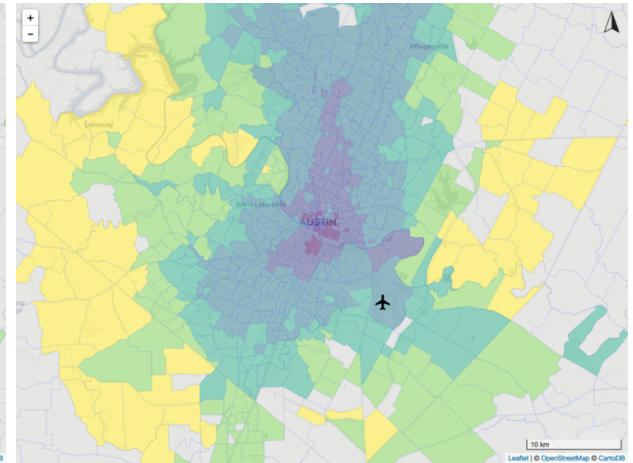
(c) Idle time data in TAZs



(d) Reach time in TAZs



(e) Idle time GFL denoised



(f) Reach time GFL denoised

Figure 3: GFL denoising examples (system-wide weekend origin trips)

found during the morning peak hour wherein we observed areas with a trip length of less than five kilometers in the downtown sector, while trips to the airport were longer. Thus, it is possible that users prefer to use ride-sourcing trips for commuting within the central area and for airport trips during morning rush hour.

Idle time provides an indirect measure of the trip supply and demand relation. It is based on the time between the end of a trip and the beginning of the next one. The results, shown based on trip origin, correspond to the idle time prior to rider pick-up at that specific location. Downtown trips present lower driver idle time than peripheral-area trips. Short idle time means that the ratio of supply-demand is near one (the demand is similar to the supply). High idle time can be attributed to low demand for rides or high driver supply, resulting in a supply-demand ratio greater than one.

The results showed a marked difference between airport trips and other TAZs trips, and this difference is constant over the time. Specifically, rides originating at the airport showed higher idle time prior to rider pick-up, suggesting that there could be an excessive driver supply in that area, causing drivers to wait longer until the next trip. However, the airport-area presented a high number of trips. Thus, it is possible that drivers are aware of the higher demand and prefer to drive there to improve the likelihood of trip assignment. We also observed a high contrast of idle times during the AM and PM peaks. Weekday evening rides tended to have a greater idle time in comparison to weekday mornings, suggesting that the supply and demand interaction of these timeframes is different. PM-peak trips present higher supply-demand ratio compared to AM-peak trips. The number of rides during weekday evenings is significantly higher compared to mornings. Thus, we can conclude that there is a considerably higher supply of drivers during the PM-peak period as compared to the AM-peak.

Reach time is the between trip assignment until the pick-up moment. This variable is an indirect measure of the driver supply in the area. Low reach-time zones have more drivers available nearby than high reach-time zones. However, reach time is also affected by driving speed and accessibility. In this study, the reach time is less than ten minutes for most of the central area, including the airport zone. However, the results present a notable difference between north-south and east-west reach time, which can be attributed to accessibility of the main north-south corridors, like Interstate Highway 35 (IH 35), State Highway Loop 1, and other arterial corridors (e.g., Lamar and Guadalupe). Considering the time discretization, morning peak-hour results show the higher variation. The north-south pattern is less than other time slots, and the low reach times are limited to within the center of the city, suggesting that accessibility to the north and south areas is limited during AM-peak hours, probably due to the delays caused by rush hour.

5.2. Productivity Variables

Productivity variables are analyzed based on the destination (drop off) TAZ of the trips, which allows us to investigate the impact of the trip destination on driver productivity. We selected only trips with origin in the CBD, representing 16 percent of the total rides evaluated. The analysis of the CBD-trip destinations provides key insights into the destination opportunity cost for drivers with similar initial conditions. The results are shown in Figure 5.

Productivity A results show an interesting relation between the very short (less than 0.8 kilometers) and long trips (more than twenty-five kilometers). For instance, based on the



Figure 4: Operational variables comparison for system-wide trips (trip origin)

AM-peak outputs, we can observe a small area of high throughput (\$60/hr-\$80/hr) of short rides within the downtown zone. Longer trips provide lower measures in the range of \$45/hr to \$55/hr, but as trips move further away from the CBD, productivity raises again to high values. This donut-like effect is also present for PM-peak, off-peak, and weekend rides, but with lesser contrast than AM-peak results. This finding may be related to the base fare that warrants a minimum fixed amount for very short trips. Thus, driver productivity for a single journey is comparable between trips of fewer than 0.8 kilometers and longer than twenty-five kilometers.

Using the measure of Productivity B, we wanted to capture the effect of the ending-zone idle time on driver productivity. The results show an interesting spatio-temporal dynamic. First, the spatial contrast is lesser than observed in Productivity A. For instance, the AM-peak results show a \$10/hr variation (from \$15/hr to \$25/hr). Also, the central area shows lower values than the periphery area. Second, the time effect is significant. For example, we can observe that Productivity B values vary significantly from the AM-peak to the PM-peak and weekend results. This suggests there it is a spatial influence in the driver productivity but that time effect has a more significant impact.

Productivity C provides insight into the productivity of two consecutive trips and takes into account the ending-zone idle time between them. In this case, results showed a lower spatial impact compared to Productivity B. Off-peak and weekend trips showed similar productivity across the majority of the area. AM-peak trips in the central region presented the most favorable productivity measure. In general, AM-peak ride results indicate that drivers who stayed in the central area ended their second trip with higher productivity compared to those who made longer trips. Regarding the time effect, weekend trips are more favorable for drivers.

6. Summary and Conclusion

This study explored the spatial structure of operational and driver performance variables in ride-sourcing using empirical data. We used information from more than 1.1 million rides in the Austin area, provided by a local TNC, from a period in which the leading companies were not operating within the city. The analysis of the operational variables, such as trip distance and search frictions, provided insights about ride-sourcing travel patterns and the balance between supply and demand across space and time. We found that during weekday AM-peak hours, riders within the central area prefer shorter trips, compared to the other time frames. Additionally, PM-peak hours tend to have significantly higher driver supply, which causes a greater supply-demand ratio compared to AM-peak. Airport-area trips showed a marked difference when compared to other Austin areas in term of operational variables, including a significantly higher amount of origin and destination rides. The results suggest that drivers prefer to drive there to warranty rides.

Furthermore, the evaluation of different productivity variables allowed the investigation of the effect of trip destination on driver productivity. Based on the results, the productivity of single trips for distances shorter than 0.8 kilometers is approximately comparable to rides longer than twenty-five kilometers. Regarding spatial effects, drivers with rides ending in the central area presented favorable spatial differences in productivity when including the revenue of two consecutive trips for AM-peak rides. However, the other time slots evaluated

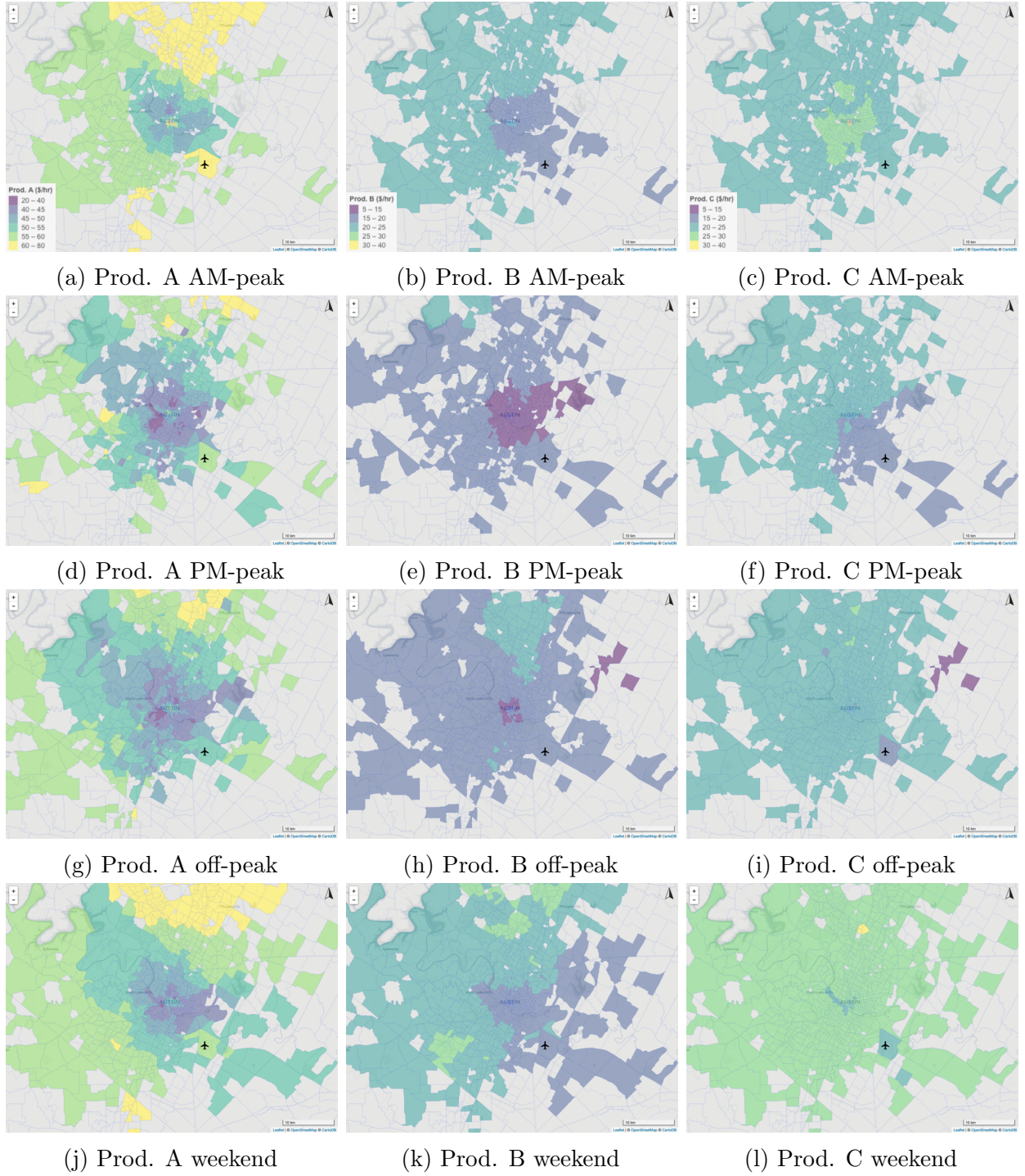


Figure 5: Productivity comparison for CBD trips (trip destination)

did not show significant differences. The time effect showed more contrast than the spatial effect, as weekend rides tend to provide better driver productivity measures.

Primary findings of this research suggest that there are differences in space and time that can affect ride-sourcing search frictions and driver productivity. Thus, providing spatio-temporal pricing strategies could be one way to balance driver equity across the network. The results and methods presented in this study can serve multiple purposes. First, from a driver and operator point of view, we identified the spatial and temporal distribution of the principal operational and productivity variables, which can lead to a more efficient driver supply method. Second, from the planners’ and engineers’ perspective, we provided insights on ride-sourcing travel patterns in the Austin area that can help to understand the characteristics of the ride-sourcing service. Third, we provide empirical evidence of driver productivity inequality due to spatial and temporal factors. This evaluation can lead to pricing strategies and policies that warranty fair conditions in driver compensation.

Finally, our results have relevance for transportation research. We provide an application of spatial smoothing to a transportation problem. This method can provide a more appropriate high-definition spatial evaluation, reduce noisy measures and enhance interpretability. Furthermore, we specifically focused on a technique that can be applied with a highly efficient and scalable algorithm that can be used with evaluations that leverage big data.

Appendix A. A Fast and Flexible Algorithm for the GFL

Tansey and Scott [35] proposed an ADMM approach to solving the GFL, where the key insight is to decompose the graph into a set of trails that can each be solved efficiently using techniques for the ordinary (1D) fused lasso. The resulting technique is both faster than previous GFL methods and more flexible in the choice of loss function and graph structure [35]. This section provides a summary of the method.

The core idea of the algorithm is to decompose a graph $\mathcal{G} = (\mathcal{V}, \mathcal{E})$ with node set \mathcal{V} of size $2k$ and edge set \mathcal{E} into a set of non-overlapping trails $\mathcal{T} = \{t_1, t_2, \dots, t_k\}$, on which the optimization algorithm can operate, and allows one to rewrite the penalty function in Equation 8 as:

$$\sum_{(r,s) \in \mathcal{E}} |x_r - x_s| = \sum_{t \in \mathcal{T}} \sum_{(r,s) \in t} |x_r - x_s| \quad (\text{A.1})$$

The updated penalty function allows proposing an efficient ADMM algorithm. The next sections present details of the updated optimization method and the trial decomposition approaches suggested by the authors.

Appendix A.1. Optimization via the ADMM

The objective function (Equation 8) can be rewritten using the updated penalty function as shown in Equation A.2. For each trail t (where $|t| = m$), we introduce $m + 1$ slack variables⁸,

⁸In an optimization problem, a slack variable is a variable that is added to an inequality constraint to transform it into an equality.

one for each vertex along the trail. Multiple slack variables are introduced if a vertex is visited more than once in a trail.

$$\begin{aligned}
& \underset{\mathbf{x} \in \mathbb{R}^n}{\text{minimize}} && \ell(\mathbf{y}, \mathbf{x}) + \lambda \sum_{t \in \mathcal{T}} \sum_{(r,s) \in t} |z_r - z_s| \\
& \text{subject to} && x_r = z_r \\
& && x_s = z_s
\end{aligned} \tag{A.2}$$

This problem can be solved using the ADMM algorithm [32] based on the following updates:

$$\mathbf{x}^{k+1} = \underset{\mathbf{x}}{\text{argmin}} \left(\ell(\mathbf{y}, \mathbf{x}) + \frac{\alpha}{2} \|\mathbf{A}\mathbf{x} - \mathbf{z}^k + \mathbf{u}^k\|^2 \right) \tag{A.3}$$

$$\mathbf{z}_t^{k+1} = \underset{\mathbf{z}}{\text{argmin}} \left(w \sum_{(r,s) \in t} (\tilde{y}_r - z_r)^2 + \sum_{(r,s) \in t} |z_r - z_s| \right), t \in \mathcal{T} \tag{A.4}$$

$$\mathbf{u}^{k+1} = \mathbf{u}^k + \mathbf{A}\mathbf{x}^{k+1} - \mathbf{z}^{k+1} \tag{A.5}$$

where u is the scaled dual variable, α is the scalar penalty parameter, $w = \frac{\alpha}{2}$, $\tilde{y}_r = x_r - u_r$ and A is a sparse binary matrix used to encode the appropriate x_i for each z_j . Here t is used to denote both the vertices and edges along trail t .

For the squared-error loss function $\ell(\mathbf{y}, \mathbf{x}) = \sum_{i=1}^n \frac{1}{2}(y_i - x_i)^2$, the x updates have the simple closed-form solution:

$$x_i^{k+1} = \frac{2y_i + \alpha \sum_{j \in \mathcal{J}} (z_j - u_j)}{2 + \alpha |\mathcal{J}|}, \tag{A.6}$$

where \mathcal{J} is the set of dual variable indices that map to x_j . Crucially, the trail decomposition approach means that each trail's z update in Equation A.4 is a one-dimensional fused lasso problem which can be solved in linear time via an efficient dynamic programming routine.

Appendix A.2. Trail decomposition

The two approaches for the trail decomposition are summarized as follows⁹:

1. Create k “pseudoedges” connecting the $2k$ odd-degree vertices and then find an Eulerian tour on the surgically altered graph. To decompose the graph into trails, we then walk along the tour (which by construction enumerates every edge in the original graph exactly once). Every time a pseudo-edge is encountered, we mark the start of a new trail.
2. Iteratively choose a pair of odd-degree vertices and select a shortest path connecting them based on an heuristic (e.g., a trail with median length). Any component that is disconnected from the graph then has an Eulerian tour and can be appended onto the trail at the point of disconnection.

⁹For a broader explanation see Tansey and Scott [35].

References

References

- [1] S. Shaheen, A. Cohen, I. Zohdy, Shared mobility: current practices and guiding principles, Technical Report FHWA-HOP-16-022, U.S. Department of Transportation, 2016. URL: <https://ops.fhwa.dot.gov/publications/fhwahop16022/index.htm>.
- [2] G. P. Cachon, K. M. Daniels, R. Lobel, The role of surge pricing on a service platform with self-scheduling capacity, *Manufacturing & Service Operations Management* 19 (2017) 368–384.
- [3] H. Ma, F. Fang, D. C. Parkes, Spatio-temporal pricing for ridesharing platforms, arXiv preprint arXiv:1801.04015 (2018).
- [4] F. He, X. Wang, X. Lin, X. Tang, Pricing and penalty/compensation strategies of a taxi-hailing platform, *Transportation Research Part C: Emerging Technologies* 86 (2018) 263–279.
- [5] K. Bimpikis, O. Candogan, S. Daniela, Spatial pricing in ride-sharing networks, Working paper, Stanford Graduate School of Business (2016).
- [6] B. Bian, Search frictions, network effects and spatial competition- taxis versus uber, Working paper, Pennsylvania State University Department of Economics (2018).
- [7] N. Buchholz, Spatial equilibrium, search frictions and efficient regulation in the taxi industry, Technical Report, Technical report, University of Texas at Austin, 2015.
- [8] L. Zha, Y. Yin, Z. Xu, Geometric matching and spatial pricing in ride-sourcing markets, *Transportation Research Part C: Emerging Technologies* 92 (2018) 58–75.
- [9] F. Castro, O. Besbes, I. Lobel, Surge pricing and its spatial supply response, Columbia Business School Research Paper No. 18-25 (2018).
- [10] H. Yang, C. Fung, K. Wong, S. C. Wong, Nonlinear pricing of taxi services, *Transportation Research Part A: Policy and Practice* 44 (2010) 337–348.
- [11] L. Zha, Y. Yin, H. Yang, Economic analysis of ride-sourcing markets, *Transportation Research Part C: Emerging Technologies* 71 (2016) 249–266.
- [12] S. Banerjee, C. Riquelme, R. Johari, Pricing in ride-share platforms: A queueing-theoretic approach, Working paper, Stanford Department of Management Science and Engineering (2015).
- [13] W. Tansey, A. Athey, A. Reinhart, J. G. Scott, Multiscale spatial density smoothing: an application to large-scale radiological survey and anomaly detection, *Journal of the American Statistical Association* 112 (2017) 1047–1063.
- [14] W. Tansey, J. Thomason, J. G. Scott, Interpretable low-dimensional regression via data-adaptive smoothing, arXiv preprint arXiv:1708.01947 (2017).

- [15] A. Samuels, Uber, lyft returning to austin on monday, Texas Tribune (2017).
- [16] J. C. Castillo, D. Knoepfle, G. Weyl, Surge pricing solves the wild goose chase, in: Proceedings of the 2017 ACM Conference on Economics and Computation, ACM, 2017, pp. 241–242.
- [17] L. Zha, Y. Yin, Y. Du, Surge pricing and labor supply in the ride-sourcing market, Transportation Research Procedia 23 (2017) 2–21.
- [18] M. Sheldon, Income targeting and the ridesharing market, Working paper, University of Chicago (2015).
- [19] M. K. Chen, M. Sheldon, Dynamic pricing in a labor market: Surge pricing and flexible work on the uber platform., in: EC, 2016, p. 455.
- [20] P. Afèche, Z. Liu, C. Maglaras, Ride-hailing networks with strategic drivers: The impact of platform control capabilities on performance, Columbia Business School Research Paper No. 18-19 (2018).
- [21] [dataset] Data World, Ride austin dataset, 2017. URL: <https://data.world/ride-austin>.
- [22] A. Chambolle, An algorithm for total variation minimization and applications, Journal of Mathematical imaging and vision 20 (2004) 89–97.
- [23] J. Yu, G. Turk, Reconstructing surfaces of particle-based fluids using anisotropic kernels, ACM Transactions on Graphics (TOG) 32 (2013) 5.
- [24] T. Tasdizen, R. Whitaker, P. Burchard, S. Osher, Geometric surface smoothing via anisotropic diffusion of normals, in: Proceedings of the conference on Visualization’02, IEEE Computer Society, 2002, pp. 125–132.
- [25] R. Compton, D. Jurgens, D. Allen, Geotagging one hundred million twitter accounts with total variation minimization, in: Big Data (Big Data), 2014 IEEE International Conference on, IEEE, 2014, pp. 393–401.
- [26] S. McLafferty, D. Williamson, P. McGuire, Identifying crime hot spots using kernel smoothing, Analyzing crime patterns (2000) 77–85.
- [27] L. Thakali, T. J. Kwon, L. Fu, Identification of crash hotspots using kernel density estimation and kriging methods: a comparison, Journal of Modern Transportation 23 (2015) 93–106.
- [28] Y.-X. Wang, J. Sharpnack, A. Smola, R. Tibshirani, Trend filtering on graphs, in: Artificial Intelligence and Statistics, 2015, pp. 1042–1050.
- [29] W. Tansey, Scalable smoothing algorithms for massive graph-structured data, Ph.D. thesis, University of Texas at Austin, 2017.

- [30] Z. D. Weller, J. A. Hoeting, et al., A review of nonparametric hypothesis tests of isotropy properties in spatial data, *Statistical Science* 31 (2016) 305–324.
- [31] R. Tibshirani, Regression shrinkage and selection via the lasso: a retrospective, *Journal of the Royal Statistical Society: Series B (Statistical Methodology)* 73 (2011) 273–282.
- [32] S. Boyd, N. Parikh, E. Chu, B. Peleato, J. Eckstein, et al., Distributed optimization and statistical learning via the alternating direction method of multipliers, *Foundations and Trends® in Machine learning* 3 (2011) 1–122.
- [33] B. Wahlberg, S. Boyd, M. Annergren, Y. Wang, An admm algorithm for a class of total variation regularized estimation problems, *IFAC Proceedings Volumes* 45 (2012) 83–88.
- [34] A. Barbero, S. Sra, Modular proximal optimization for multidimensional total-variation regularization, *arXiv preprint arXiv:1411.0589* (2014).
- [35] W. Tansey, J. G. Scott, A fast and flexible algorithm for the graph-fused lasso, *arXiv preprint arXiv:1505.06475* (2015).